

# Ultrafast Holographic Recording Using Two-Photon Induced Photopolymerization

Sean M. Kirkpatrick, Lisa R. Denny, Morley O. Stone

Materials and Manufacturing Directorate, Air Force Research Laboratory, Wright-Patterson Air Force Base, OH 45433

## ABSTRACT

Previously, we have reported the first demonstration of holographic two-photon induced photopolymerization (H-TPIP) in the construction of transmission holograms. This technique relies on the coupling of a two-photon absorbing chromophore and a photocurable optical resin. Several different systems have been successfully explored; all involving varied reaction pathways. Since the initial report, we have also expanded this technique to reflection holograms and some bulk structures. While the applications for this process are widely ranging, the underlying physical mechanisms still require a great deal of investigation. In this work, we report on some of the photo-physical mechanisms involved in the H-TPIP technique. Specifically, we will report on evidence for mass-transport phenomena, and the role of localized thermal loading. We also discuss a preliminary model, which examines the coupling between the chromophore's excited state population, initiation of the polymerization reaction, and localized thermal deposition.

**Keywords:** holographic, two-photon absorption, femtosecond, excited state, photopolymerization, ultrafast

## 1. INTRODUCTION

The first demonstration of ultrafast holographic two-photon induced photopolymerization (H-TPIP) has recently been reported in the construction of transmission diffraction gratings<sup>1</sup>. Where as traditional, one-photon induced polymerization is well understood and has become an integral part of high precision processing, (such as MEMS manufacturing<sup>2</sup>) two-photon induced polymerization (TPIP) has been studied to a lesser extent. However, TPIP has appeal as a method for the fabrication of 3D sub-micron structures including 3D optical data storage devices and photonic band-gap structures<sup>3</sup>. It has previously been shown that two-photon induced photopolymerization has application in lithographic microfabrication<sup>4,5,6</sup> where use is made of a confocal region of a focused beam to confine the two-photon absorption to a volume on the order of  $\lambda_0^3$ , where  $\lambda_0$  is the wavelength of incident radiation<sup>7</sup>. Until recently, as illustrated by two-photon-based optical data storage<sup>8</sup>, it was necessary to sequentially scan a series of high peak-intensity laser pulses in a tightly-focused single-beam geometry in order to cross the TPIP initiation threshold within the focal region, and form the desired structure via a pixilated, serial generation process. H-TPIP accomplishes this process without the need for a confocal single beam, representing a parallel form of photopolymer processing compared to the serial technique used previously.

In order to accomplish a holographic form of microfabrication via this technique, it is necessary to use initiating chromophores that have a high two-photon absorption cross section. In particular, several systems have been explored having various reaction pathways (with and without co-initiators) and/or physical attributes (water-soluble, naturally occurring or synthesized)<sup>9</sup>. For the purposes of this work, we will focus solely on an Air Force chromophore AF380, and a commercial resin, NOA 72™. AF-380 represents a multi-dimensional version of a class of linear, asymmetric two-photon chromophores under examination within the Air Force Research Laboratory. These molecules consist of a  $\pi$ -electron donating and accepting moieties separated by a conjugated aromatic bridge (D- $\pi$ -A)<sup>10,11,12</sup>. Due to patent issues, the exact chemical structure can not yet be disclosed. However, in comparison to other dyes that have been previously reported, AF380 has a larger molecular weight, a three-fold increase in linear molar absorption coefficient, and a 30 nm shift in peak linear absorption of the lowest energy transition. For the linear dye analogs, a similarity of absorbance spectral features for a series of dyes with different  $\pi$ -electron accepting species suggested that the excitation was centered on a common subset of the molecules, namely the D- $\pi$  portion of each molecule. This was further supported through the observed sensitivity of the fluorescence to the nature of the

$\pi$ -electron accepting species. Because AF-380 shares this same D- $\pi$  portion and has a similar, yet red-shifted, linear absorbance spectrum, the increase in conjugation length may be centered on the multi-dimensional D- $\pi$  portion of the molecule.

Our initial report demonstrated the recording of transmission diffraction gratings by combining two femtosecond pulses of near-infrared light within a film of the above material system. Since first reporting this process, we have been studying the physics and behavior of this system in depth. Particularly, we were intrigued by the hypothesis that the grating structure is actually formed by mass transport of monomer to polymer. This report updates the progress we have made in writing reflection gratings as well as other more complex structures. We also report on progress in modeling the grating-formation kinetics and some of the contributing mechanisms.

## 2. EXPERIMENTAL

### 2.1. Film Fabrication

For the formation of transmission grating patterns via H-TPIP, thin films were fabricated by spin-coating a 0.4 wt.% blend of the two-photon absorbing chromophore AF380 in NOA 72 onto polystyrene and glass slides using a commercially available spincoater. To ensure solubility and dispersion of the chromophore within the monomer matrix, the chromophore was dissolved in a small amount of benzene prior to blending (~5% benzene by volume in final solution). The NOA 72 was passed through a 2  $\mu\text{m}$  filter prior to mixing with the chromophore. The final solution was then re-filtered immediately prior to spin coating. Films were ~ 10  $\mu\text{m}$  thick as determined by SEM cross-section. For the formation of reflection-type holograms via H-TPIP, thin films were fabricated by pressing a 0.4 wt.% blend of the two-photon absorbing chromophore AF380 in NOA 72 between glass slides using commercially available Teflon spacers. Film thickness varied with the type of Teflon spacer used. A spacer thickness range of 15 microns to 500 microns was used. These spacers were inserted between two microscope slides, filled with the above mixture, and sealed at the edges.

### 2.2. Optical Configuration

The optical setup used to write the grating structures was a two beam holographic configuration. A Ti:Sapphire femtosecond laser system with regenerative amplification was used to generate a bandwidth limited ultrafast (typically 90 fs) pulse in the infrared (700-900 nm). High intensity, low dispersion optics were used throughout the experimental arrangement. The spot size was reduced from a square centimeter to 5 mm<sup>2</sup> using a pair of thin lenses in a telescope arrangement, and the beam was split into two pulses using an ultrafast beam splitter. It is important to note that the relative energies of the two pulses are not equal. The weaker of the two pulses is used for the patterning, while the more energetic pulse allows us to reach the threshold value for initiation of the process. This ratio is different per material system. Each of the two beams was propagated along optical delay lines, one of which was a variable translation stage with a resolution of 30 fs/step. For transmission type holograms, the two beams were incident on the sample plane at an angle of  $\phi^\circ$  to the normal, subtending an angle of  $2\phi^\circ$  between them. The grating spacing is then defined in the usual manner ( $\Lambda = \lambda_0 / (2\sin(2\phi))$ ). For reflection type holograms, the beams are nearly counter-propagating giving a grating spacing of  $\lambda_0$ . As the coherence length of each pulse is approximately 30  $\mu\text{m}$ , care must be taken to ensure accurate temporal and spatial overlap. To ensure temporal overlap, a KDP crystal is placed in the sample plane and the translation stage moved until the maximum of the second harmonic generation signal is determined. This process has the advantage of allowing us to also autocorrelate the pulse at the sample plane. An alternative method used is a thin film of a two-photon absorbing dye which upconverts the fundamental pulses to a visible wavelength. Zero time overlap is then found by observing the bright flash of nonlinear fluorescence. By maximizing the temporal overlap, we also force the two beams into coherence with respect to each other. In addition, both the KDP crystal (TPA dye) and the sample holder are mounted on a rail to ensure that the interaction plane was identical by sliding either one or the other into the overlapping beams. The energy of each pulse is attenuated using a variable thin neutral density filter, and is measured at the sample plane using a calibrated power meter. Both the energy and beam size is chosen to give an appropriate intensity distribution about the threshold intensity. Exposure times are determined by the kinetics of the reactions and can vary from as little as tens of seconds to as long as a few minutes. Although the grating spacing is determined from the subtended angle, the actual peak to valley dimension (Z) is determined by the intensity distribution about threshold of the generated pattern. To date, we have demonstrated a 50 nm peak to valley height, with large area patterns covering several mm<sup>2</sup>.

### 2.3. Optical Characterization

Once fabricated, holograms were examined using a CCD camera to record image formation in either transmission or reflection geometries at either 632.8 nm or using a white light source. In addition, transmission spectra of holographic gratings were obtained using an Ocean Optics fiber coupled spectrophotometer.

#### 2.4. Film Morphology and Kinetics

Intensity dependent film thickness data were obtained using a Dektak IIA profilometer. The time dependent formation of the films was measured by propagating a low power HeNe through the center of the film during the writing process. A silicon photodiode and A/D converter was used to collect real time transmission data during the formation of the photo-induced polymer film. Several sets of data were then collected as a function of pump intensity.

#### 2.5. Chromophore Excited State Dynamics

The excited state dynamics of AF380 were measured using transient white light absorption spectroscopy. The experiment and results are presented elsewhere and so only relevant data are highlighted as needed<sup>13</sup>. In addition, a preliminary rate model of this chromophore is also presented in the same reference.

#### 2.6. Thermal Load Measurements

Thermal expansion of the chromophore/resin system was observed using a capillary melting point apparatus. Capillary tubes with one end sealed were used as sample holders, having interior diameters of 1.1 mm. The Norland 72/AF-380 system was injected into the tubes so that the height of the solution was approximately 4 mm; the filled tubes were left to sit overnight to allow the viscous solution to flow to the bottom. A Bausch and Lomb reticulated eyepiece was used to measure the exact height of the column of solution prior to heating. The melting point apparatus was heated to the desired temperature and allowed several minutes to equilibrate at temperature prior to measurement. The sample was placed in the melting point apparatus to heat for 2 minutes. The heated tube was removed and the height of the solution was measured immediately to determine the extent of fluid expansion at that temperature. A total volume expansion of 1-2% was observed in samples heated in the range of 30-40 °C. Samples heated to 100 °C exhibited thermal expansion values of approximately 10% accompanied by partial curing of the system. In addition, a thin film of thickness 100 µm was also prepared with a J type thermocouple wire incorporated into the material system. The increase in bulk temperature was measured at the center of the laser spot in a similar configuration as that used to obtain reflection holographic images with the exception of using the full pulse energy of 1 mJ. In this manner, a comparison to thermally induced polymerization could be obtained. Using this technique, a 10 °C increase in temperature to 34 °C was observed.

### 3. RESULTS AND DISCUSSION

Our initial transmission grating results, as reported earlier, are summarized in Table 1. Since that time, we have reduced the transmission grating spacing to around 800 nm, begun quantifying the system parameters for accurate modeling of complex patterns, and recorded several Bragg reflection gratings covering nearly a square centimeter.

We have also demonstrated that the polymerization is truly a two-photon process by measuring the film thickness as a function of intensity. Shown in Figure 1 is a plot of polymer thickness versus pulse energy under identical conditions. As can be seen from the solid line, these data fit to a pure quadratic dependence as expected for such a two-photon assisted process.

Expanding the transmission holographic technique, we have recorded several holographic reflection gratings using a nearly counter-propagating geometry. The appropriate reflection notch (at the writing wavelength of 800 nm) and a CCD image of the near-normal incidence holographic reflection from a 200 µm thick film is shown in Figure 2. Note that as the total spatial overlap of the counter-propagating pulses is ~30 µm along the propagation axis, and that the film thickness is 200 µm, this image represents the construction of a reflection grating within a bulk sample. This fact will need to be verified using SEM analysis. The total area covered by the grating is now 4 mm<sup>2</sup>, while the diffraction efficiency is about 15%. While this represents an increase in the size of the image formed, the diffraction efficiency is not optimal at this time.

In order to make this technology useful for specific applications, it is necessary to understand the photophysical mechanisms responsible for the structure formation and then to combine this understanding with careful control over the

Grating Spacing	3.8 µm
Peak to Valley Height	50 nm
Peak Diffraction Efficiency	40 %
Area	1 mm <sup>2</sup>

**Table 1 Summary of previous results describing transmission gratings formed via H-TPIP.**

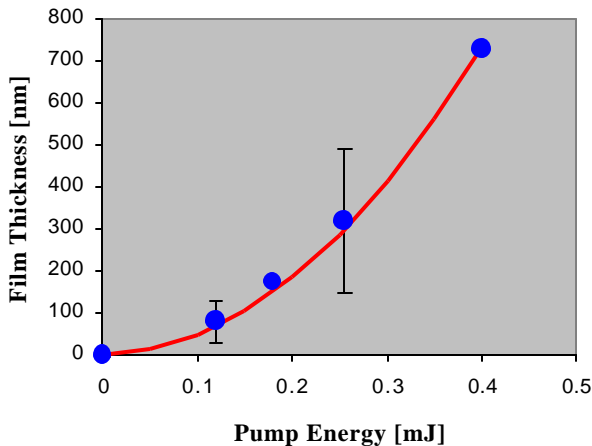


**Figure 1** Film thickness as a function of pulse energy.

associated with the ESA occurs at all pump intensities where two-photon absorption occurs. The time development of the excited state dynamics was shown to include an intermediate state in the dynamics associated with a lower ESA cross section. It was also found that the longer time scale ESA is associated with absorption to the continuum allowing for nearly free electrons. The transient absorption spectra resulting from that study are shown in Figure 4. Note the drop in ESA around 500 picoseconds associated with the intermediate transitional state having a lower excited state cross section. The subsequent slow rise across the entire spectrum is attributed to absorption to a long-lived state; most likely to the continuum population based on energy conservation and molecular quantum calculations of this molecule<sup>13</sup>. It is this excited state absorption and subsequent longer lived state that is believed to affect nanosecond measurements of the two-photon absorption cross section. Attempts at optically inducing the photopolymerization reaction via nanosecond excitation at comparable intensities and wavelength failed to produce any curing in this system. These facts combined, lead us to the

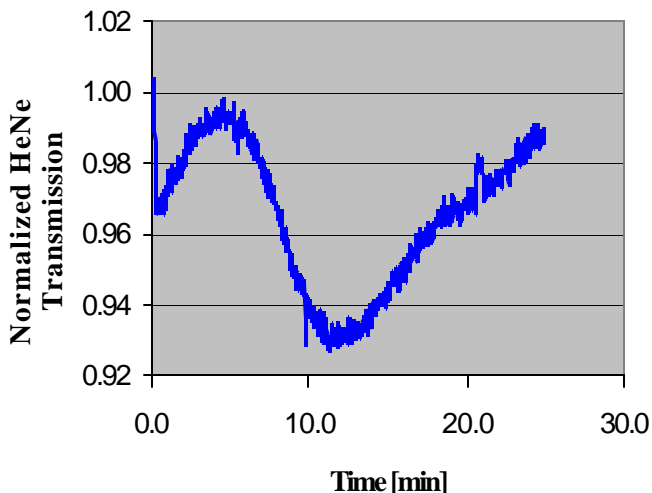


**Figure 3** HeNe transmission versus time through a 10 micron film during a H-TPIP process.

phase and intensity profile of the short pulsed lasers needed to reach the intensities required. Therefore, in beginning to quantify the mechanisms responsible for the formation of a grating, we have discovered a very rich and complicated chain of events, which will require further study. Presented in Figure 3 is a temporal measurement of the transmission of a helium-neon laser through the center region of a 10  $\mu\text{m}$  film during the writing of a grating pattern. The relative mean intensity of the interference pattern is approximately half of what is typically used in order to slow down several of the visible processes. The first feature visible at zero time is an instantaneous drop in the transmission of the HeNe. This is believed to be due to excited state absorption (ESA) out of the initial two-photon excited state. A separate study on this process alone has been presented elsewhere<sup>13</sup>. It was shown in that work that the instantaneous drop in transmission

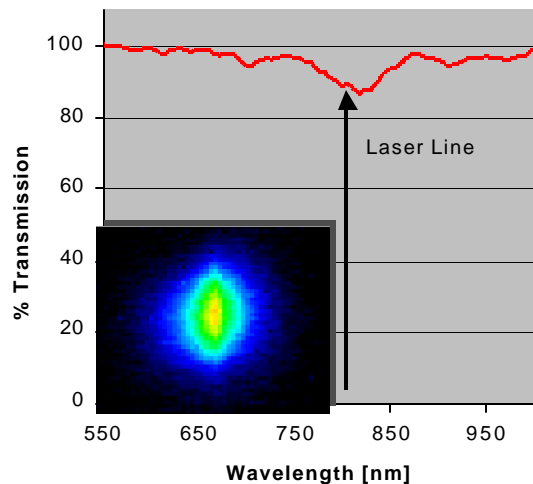


**Figure 2** Reflection notch and holographic image of reflection grating written at 800 nm.

conclusion that the two-photon excited state is the initiating population of the photopolymerization, and that any decrease in that population via ESA or quenching leads to an inhibition of the photopolymerization reaction.

Returning to Figure 3, the gradual increase in the transmission following the initial ESA can be attributed to a thermal relaxation of the viscosity of the film and a slow thinning of the film thickness in response to the thermal load. Considering the thermal experiments detailed above, it has been seen that laser irradiation at the typical peak intensities used in our work, results in a column expansion of several percent. For the case of an unconfined film, one would expect that the thermal expansion will occur in the plane, and thus should thin the film, consistent with observation. The most likely source of the thermal load comes from the nonradiative relaxation of the two-photon excited state to the nearby one-photon excited state, as well as intramolecular relaxation within the singlet manifold. Due to the close coupling of the one- and two-photon

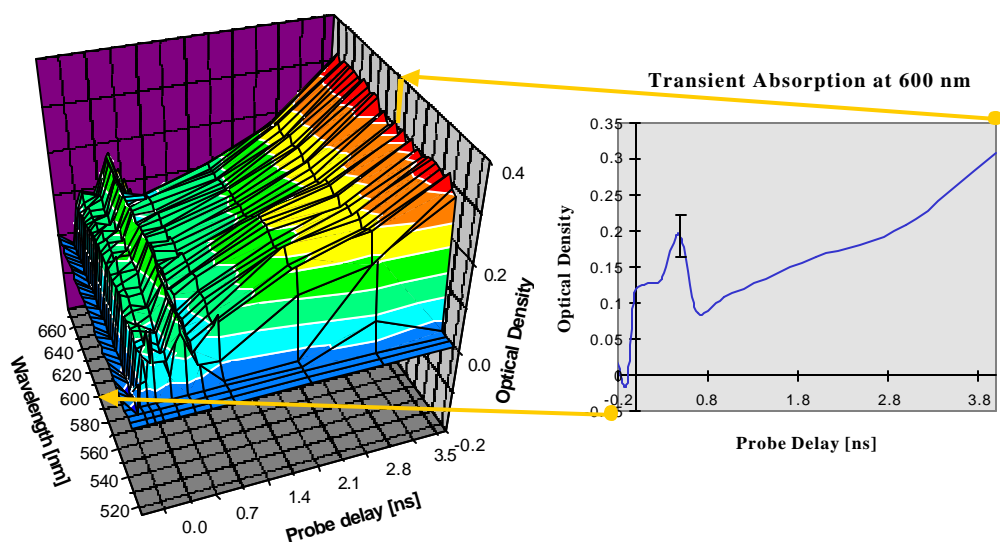


**Figure 4** Transient white light absorption spectrum of AF380 in THF.

excited states, one would expect that the total phonon emission would not be very much, as is indicated by the low temperature increase measured in the film.

The ensuing large decrease in transmission is believed to be the beginning formation of oligomers and the subsequent cross-linking to form polymer. Visual inspection of the film during this time shows a welling up of the material forming a

lens type structure, indicating mass transport. The slow increase in the transmission at long times may be associated with the process running out of material and slowly relaxing into a polymer film of uniform thickness, with the possibility of evolving excited state dynamics playing a significant role. As the pulse energies are increased (and the corresponding intensities increased) the dip in transmission corresponding to polymer formation moves to the left in time, and eventually occurs nearly instantaneously (see Figure 5). At these intensities, the polymer formation occurs much faster than the thermal relaxation making structure formation effectively thermally isolated as the exposure time can be reduced to essentially a few seconds or less. It should be reiterated that thermal initiation of the polymerization reaction did not fully occur until near 200 °C without any observed mass transport, and that the laser induced a temperature increase of only 10 °C above room temperature.

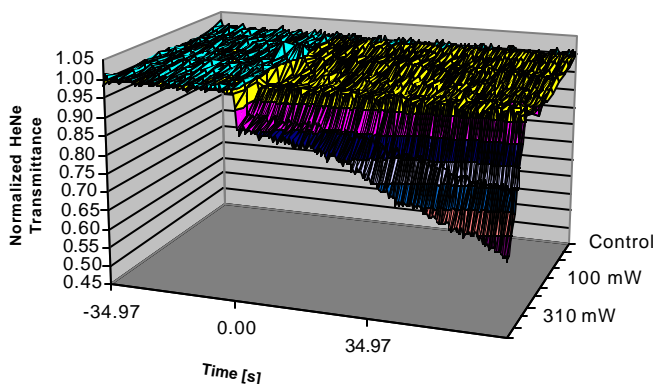


**Figure 5** Transmission of probe beam during polymer formation as a function of increasing pump power indicating the ESA, slow thermal relaxation, and polymer formation.

## 4. CONCLUSIONS

We have demonstrated that using a dye with a very large two-photon cross-section and a commercially available photopolymer, the process of two-photon-induced polymerization can be spatially controlled by using both reflection and transmission type holographic techniques from a femtosecond laser. H-TPIP has been extended from forming transmission type diffraction gratings to reflection type diffraction gratings. While previous results indicate that structure sizes on the order of nanometers are possible, and a concurrent paper discussing biomimetic applications explores feature sizes<sup>14</sup>, this work primarily focuses on forming a preliminary model for describing this process. It is believed that there are three main processes involved in structure formation. These are excited state dynamics, thermal emission, and mass transport resulting from the polymerization reaction. Evidence concerning the excited state dynamics suggests that the initiating state is the singlet-state that is closely coupled to the two-photon excited state. Long pulse photo-initiation, which effectively removes population from this manifold, fails to produce curing. Thermal curing fails to produce any observable mass transport, however, can account for the short time scale decrease in viscosity and thinning of an unconfined film. In addition, it has also

been shown that the photopolymerization step results in mass transport, which effectively thickens the high intensity regions of the film. This transport phenomenon appears to occur quicker in the higher intensity regions, and can overcome thermal effects. Future work will focus on quantitatively modeling the system with the aim to accurate prediction of the wave front parameters in order to produce desired structures in both 2 and 3 dimensions. We believe that such parallel writing of multi-dimensional structures will have a significant impact on current usage of TPIP technologies for data storage, MEMS, NEMS, and biotechnology.

## ACKNOWLEDGEMENTS

The authors wish to thank Jeff Baur and Casey Clark for their contributing efforts and continuing collaborations. We would also like to thank the Air Force Office of Scientific Research for sponsoring the work of M.O.S. and the synthesis of two-photon absorbing chromophores under contract F4962093C0017. This work is part of an ongoing collaboration between the polymer and biotechnology groups in AFRL/ML.

## REFERENCES

- 1 S. M. Kirkpatrick, J. W. Baur, C. M. Clark, L. R. Denny, D. W. Tomlin, B. R. Reinhardt, R. Kannan, M. O. Stone, *Rapid Comm. Appl. Phys. A* **69**, 461 (1999).
- 2 J. D. Bhawalker, G. S. He, and P. N. Prasad, *Rep. Prog. Phys.* **59**, p. 1041 (1996).
- 3 R. A. Borisov, G. N. Dorojkina, N. I. Koroteev, V. M. Kozenkov, S. A. Magnitskii, D. V. Malakhov, A. V. Tarasishin, A. M. Zheltikov, *Appl. Phys. B* **67**, p. 765 (1998).
- 4 B. Crumpston *et al.*, *Nature* **398**, p. 51 (1999).
- 5 S. Maruo, O. Nakamura, S. Kawata, *Opt. Lett.* **22**, p. 132 (1997).
- 6 S. Mauro, S. Kawata: *J. Microelectromechanical Systems* **7**, p. 411 (1998).
- 7 C. Xu and W. W. Webb in *Topics in Fluorescence Spectroscopy Vol. 5 – Nonlinear and Two-Photon Induced Fluorescence*, edited by J. R. Lakowitz, p. 509 (Plenum Press, NY, NY 1997).
- 8 J. Strickler, W. Webb, *Opt. Lett.* **16**, p. 1780 (1991).
- 9 Dr. Morley Stone, personal communication.
- 10 Bruce A Reinhardt, Lawrence L Brott, Stephen J. Clarson, Ann G. Dillard, Jaayprakash C. Bhatt, Ramamurthi Kannan, Lixiang Yuan, Guang S. He and Paras N. Prasad *submitted Chemistry of Materials* (1998).
- 11 Jeffery W. Baur, Max D. Alexander Jr., Michael Banach, Lisa R. Denny, Bruce A. Reinhardt†, and Richard A. Vaia Paul A. Fleitz, Sean M. Kirkpatrick, *submitted Chemistry of Materials* (1999)
- 12 Jeffery W. Baur, Max D. Alexander Jr., Richard A. Vaia and, Sean M. Kirkpatrick, manuscript in preparation.
- 13 Sean M. Kirkpatrick, Casey M. Clark, and Richard R. Sutherland, *Proc. MRS* (1999).
- 14 Current SPIE proceedings, LA 3934-12.